ELSEVIER

Marine Geology 186 (2002) 541–555

MARINE GEOLOGY
INTERNATIONAL JOURNAL OF MARINE GEOLOGY, GEOCHEMISTRY AND GEOPHYSICS

www.elsevier.com/locate/margeo

Late Cenozoic sedimentary environments in the Amundsen Basin, Arctic Ocean

K.T. Svindland, T.O. Vorren *

Department of Geology, University of Tromsø, N-9037 Tromsø, Norway

Received 15 May 2001; accepted 8 February 2002

Abstract

Analyses of sediment cores recovered on the Arctic '91 cruise with RV *Polarstern* to the Amundsen Basin and Lomonosov Ridge identify four main sedimentary facies and associated depositional sedimentary processes. These include: (1) homogenous mud facies interpreted as hemipelagic deposits, most abundant in the central parts of the Amundsen Basin; (2) fining upward cycle facies interpreted as fine-grained distal turbidite deposits, present in all Amundsen Basin cores, but most abundant laterally in the basin; (3) massive diamicton facies, found in the North Pole core; and (4) laminated diamicton facies, abundant in the upper parts of Lomonosov Ridge cores. Both diamictons are heavily influenced by ice-rafted debris, and the massive diamicton may result from redeposition of laminated diamicton downslope from the Lomonosov Ridge. The Lomonosov Ridge core exhibits a sedimentation rate of 29 mm/ka, while the sedimentation rates of turbidite rich sediments of the Amundsen Basin may be up to 10 times as high. Clay minerals show that the eastern Kara Sea and the Laptev Sea is the source area for most of the sediments, while some clay mineral zones may have their source in northern Greenland or the Barents Sea shelf.

Keywords: Arctic Ocean; sediment facies; sedimentation rates; turbidites; clay mineralogy

1. Introduction

1.1. Background

Unlike other deep-sea oceans, the Arctic Ocean (Fig. 1) is covered by sea-ice, a situation that is supposed to have lasted for several million years through the Cenozoic. Several different theories of how and when the ice cover was initiated exist (Clark, 1990). Drifting ice, both sea-ice and glacial icebergs, are sediment transport agents unique to high latitude seas, giving ice-rafted sediments as a characteristic feature. ODP leg 151 (Wolf-Welling et al., 1996) indicates pulses of ice rafting in the Fram Strait since 14 Ma BP, and more continuous ice-rafted debris (IRD) deposition and continuous sea-ice reaching the Fram Strait since between 1.9 and 1.2 Ma. However, there are also other types of sedimentary processes in the deep Arctic Ocean Basin that have not been much studied. In fact, our result show that the bulk of the sediments are derived from gravity flow processes.

Based on palaeomagnetic studies from the

* Corresponding author. Fax: +47-7764-5600.
E-mail address: torev@ibg.uit.no (T.O. Vorren).

0025-3227/02/$ – see front matter
PII: S0025-3227(02)00197-4

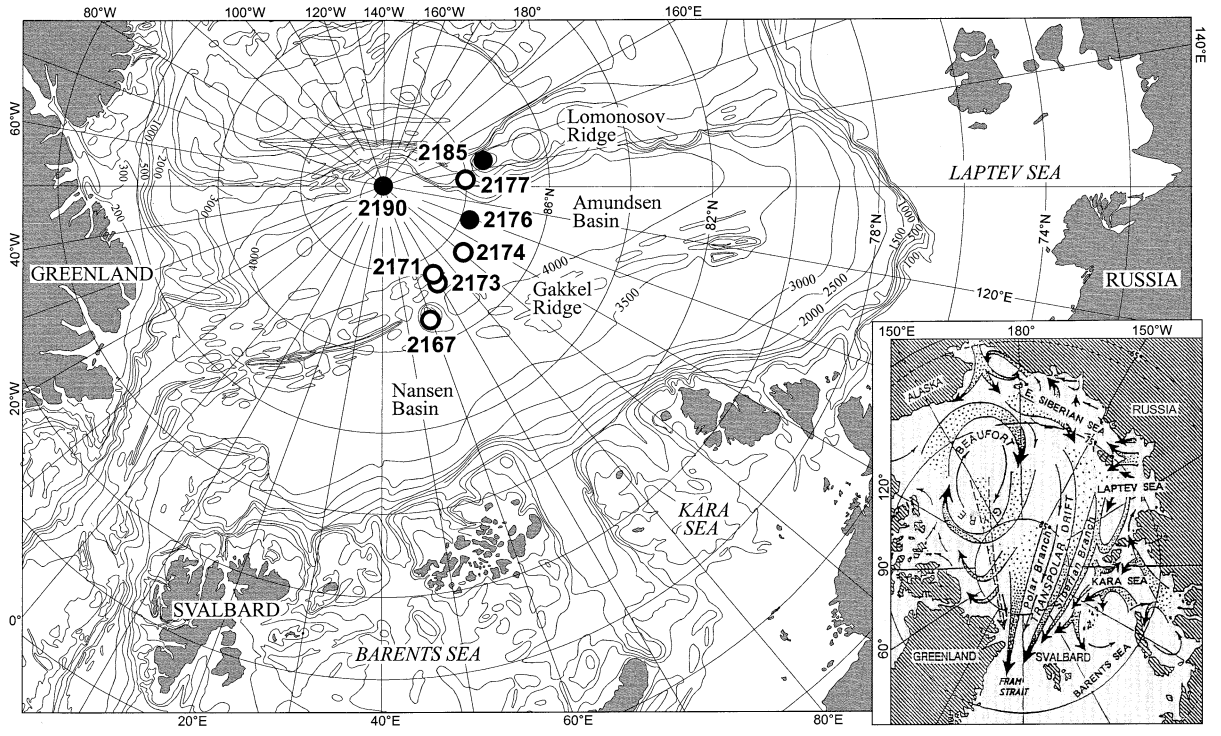

Fig. 1. Location map and bathymetry of the study area. Filled circles indicate cores sampled and studied in detail, open circles indicate cores studied from photos, X-radiographs and shipboard logs. Inserted map shows the Arctic Ocean with major current systems from Gordienko and Laktionov (1969).

Amerasian Basin, sedimentation rates of the Arctic Ocean have traditionally been considered low, 1–5 mm/ka (Clark et al., 1980; Herman and Hopkins, 1980). Sejrup et al. (1984) suggested from amino acid epimerisation data sedimentation rates 10–50 times higher. Darby et al. (1997) differentiate the sedimentation rate between 5 mm/ka for glacial regimes and 10–20 mm/ka for interglacial regimes. Grantz et al. (1996) conclude with sedimentation rates ≤ 10 mm/ka in pelagic/IRD sedimentation environments, but have found sedimentation rates as high as 1200 mm/ka in turbidite deposits of the Canada Abyssal Plain.

This study is concentrated on the sediments in the Amundsen Basin and the adjoining Lomonosov Ridge. Our objective is to identify the origin of the sediments with respect to provenance and transport/sedimentation processes. Furthermore, we will assess the sedimentation rate and compare it to previous studies.

1.2. Physiography

The Arctic Ocean is subdivided into basins by ridges as shallow as about 1000 m water depth. The Lomonosov Ridge separates the Amerasian Basin and the Eurasian Basin. The Eurasian Basin is subdivided into the Nansen Basin and Amundsen Basin by the mid-oceanic Gakkel Ridge (Johnson et al., 1990) (Fig. 1). The deep-sea floor of the Amundsen and Nansen Basins are at depths between 3000 and 4500 m (Jakobsson, 2000).

Ocean surface currents in the Eurasian Basin (Fig. 1) include the Transpolar Drift, flowing from the Siberian shelf (particularly the Laptev Sea) to the Fram Strait, and fed by several minor currents flowing off the Siberian shelves. The Amerasian Basin is dominated by the clockwise flowing Beaufort Gyre (Gordienko and Laktionov, 1969). The Beaufort Gyre and the Transpo-

lar Drift have existed since at least the late Pleistocene according to Phillips and Grantz (2001).

Bottom currents and possible intermediate currents are less well known. The sparse data available suggest both intermediate and bottom currents moving in directions independent of the surface currents (Jones et al., 1995). Aagaard and Carmack (1994) have indicated a subsurface circulation with boundary currents anti-clockwise along the slopes of the Amundsen Basin.

Shallow epicontinental seas surround the Arctic Ocean. Presently, sediment is fed onto the Arctic Ocean shelves by large rivers flowing northwards, mainly on the Asian side, but also on the Canadian side (Johnson et al., 1990). Sediment loaded sea-ice drifting with the surface ocean currents from the shelves are important transport agents for sediments to the central Arctic Ocean (Nürnberg et al., 1994; Pfirman et al., 1995, 1997).

2. Materials and methods

The investigation is based on eight kastencores (Fig. 1 and Table 1) collected on RV *Polarstern* during the 1991 cruise to the Arctic Ocean (Fütterer, 1992).

Description of the cores 2176-3 and 2190-1 was conducted parallel to description of scale 1:1 X-radiographs. Sedimentary boundaries and structures were classified according to Eidnes (1993). The other six cores were described based on colour photos and X-radiographs, with the shipboard logs and descriptions (Fütterer, 1992) as an additional source of information. One of these cores, 2185-6, is used extensively in further discussions in this paper. The general stratigraphy and sedimentary facies of all cores are shown on Fig. 2.

The cores 2176-3 and 2190-1 were sampled at irregular intervals. The sampling strategy aimed to provide both an overall stratigraphic representation of the core, and to give a detailed high resolution representation of selected individual sedimentary facies and depositional cycles; sampling intervals may be as small as 0.5–1 cm to get high resolution data from selected sedimentary cycles.

Samples from cores 2176-3 and 2190-1 were disperged and cleaned of organic matter in a 10% H_2O_2 solution, wet sieved at 63 μm, and clay (<2 μm) was separated from silt in Atterberg (sedimentation) cylinders. Fractions were dried and weighed to give the sand–silt–clay distribution. The grain-size distribution within the silt fraction was analysed with a Micromeritics Sedigraph 5100 as described by Stein (1985).

Silt samples from core 2185-6 were made available for Sedigraph analyses by Alfred Wegener Institut, together with sand–silt–clay distribution results.

Oriented clay fraction samples from cores 2176-3 and 2190-1 were analysed in a Philips 1700 X-ray diffractometer with cobalt Kα-X-ray source. To get results comparable to other studies in the same region, analyses and interpretation were performed as described by Stein et al. (1994) which identifies the following four clay minerals and their semiquantitative percentage of the clay fraction (<2 μm): smectite, illite, kaolinite, and chlorite. Clay mineralogy from core 2185-6 was obtained from Spielhagen et al. (1997).

Table 1
Location, length and depth of cores

Core number	Latitude	Longitude	Location	Metres below sea level	Core length (m)
2190-1	90°N		Amundsen Basin, near Lomonosov Ridge	4275	4.27
2185-6	87°32.2′N	144°55.6′E	Lomonosov Ridge	1052	8.20
2177-5	88°2.1′N	134°36.7′E	Lomonosov Ridge	1400	6.94
2176-3	87°46.3′N	108°23.6′E	Amundsen Basin	4364	9.76
2174-5	87°29.1′N	91°32.6′E	Amundsen Basin	4427	9.60
2173-1	87°18.4′N	69°19.3E	Amundsen Basin	4558	5.50
2171-4	87°36.1′N	69°22.8′E	Amundsen Basin	4395	3.25
2167-1	86°56.7′N	59°0.9′E	Amundsen Basin	4434	6.40

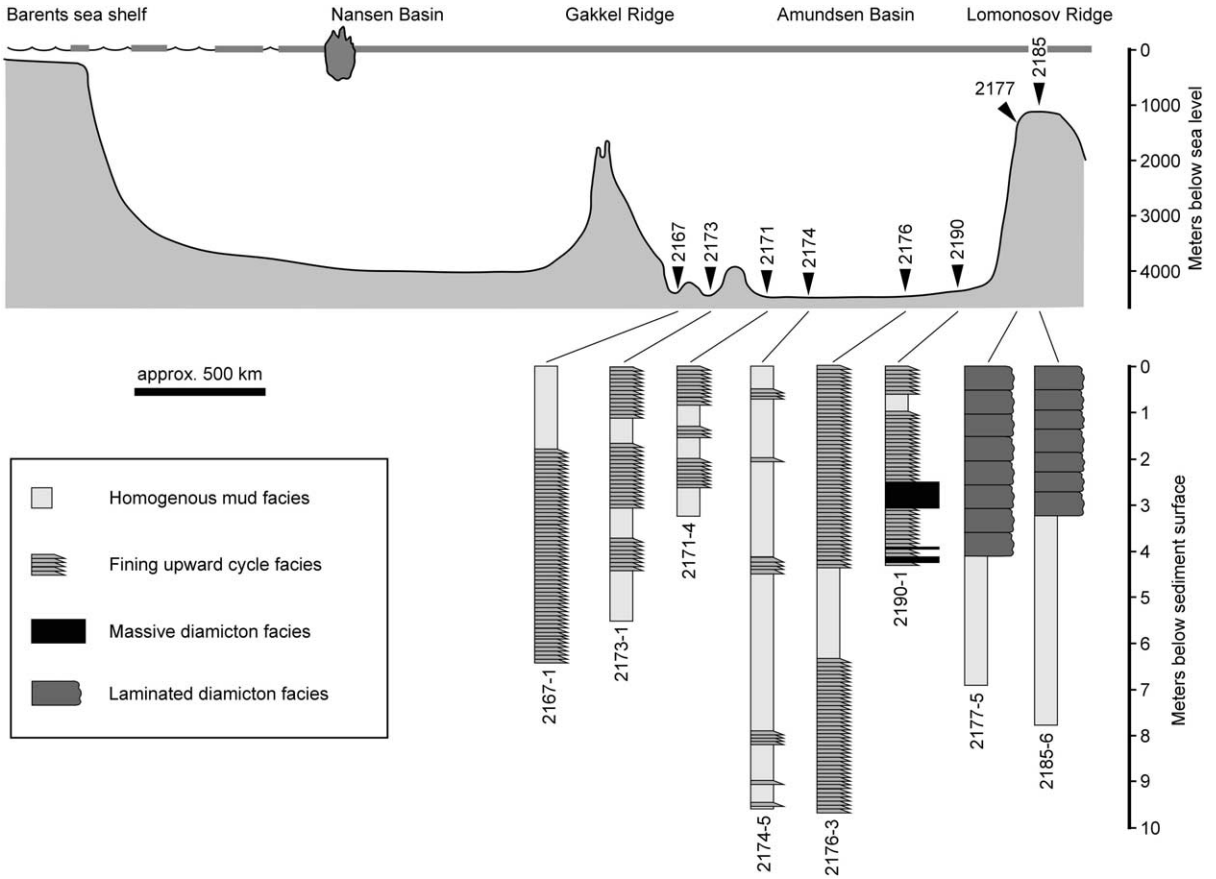

Fig. 2. Schematic bathymetric profile from the Barents Sea continental shelf through Nansen and Amundsen Basin to the Lomonosov Ridge. Core locations are indicated, and sedimentary facies of the cores are included.

Frequency of IRD was provided from AWI's databases (personal communication, Hannes Grobe). The frequency is estimated by counting grains larger than 2 mm at 1-cm intervals crossing an X-radiograph of a 10-cm-wide, 1-cm-thick core slab (Grobe, 1987).

3. Results

3.1. Sedimentary facies

Four main sedimentary facies are identified, consisting of homogenous mud facies, fining upward cycle facies, massive diamicton facies, and laminated diamicton facies (Fig. 2).

3.1.1. Homogenous mud facies

This facies comprises sediments dominated by clay. Sand and IRD are absent or scarce in the basin cores. Laminations and fining upward texture (normal grading) may occur, but are scarce. This sediment facies dominates the deep parts of the Amundsen Basin. It is present in all cores of the Amundsen Basin, but is most abundant in core 2174-5 in the central part of the basin. This facies is also identified in cores on the Lomonosov Ridge, with higher presence of IRD, and 3–7% sand.

3.1.2. Fining upward cycle facies

This facies is dominated by clay and fine to medium silt. Most samples contain only traces

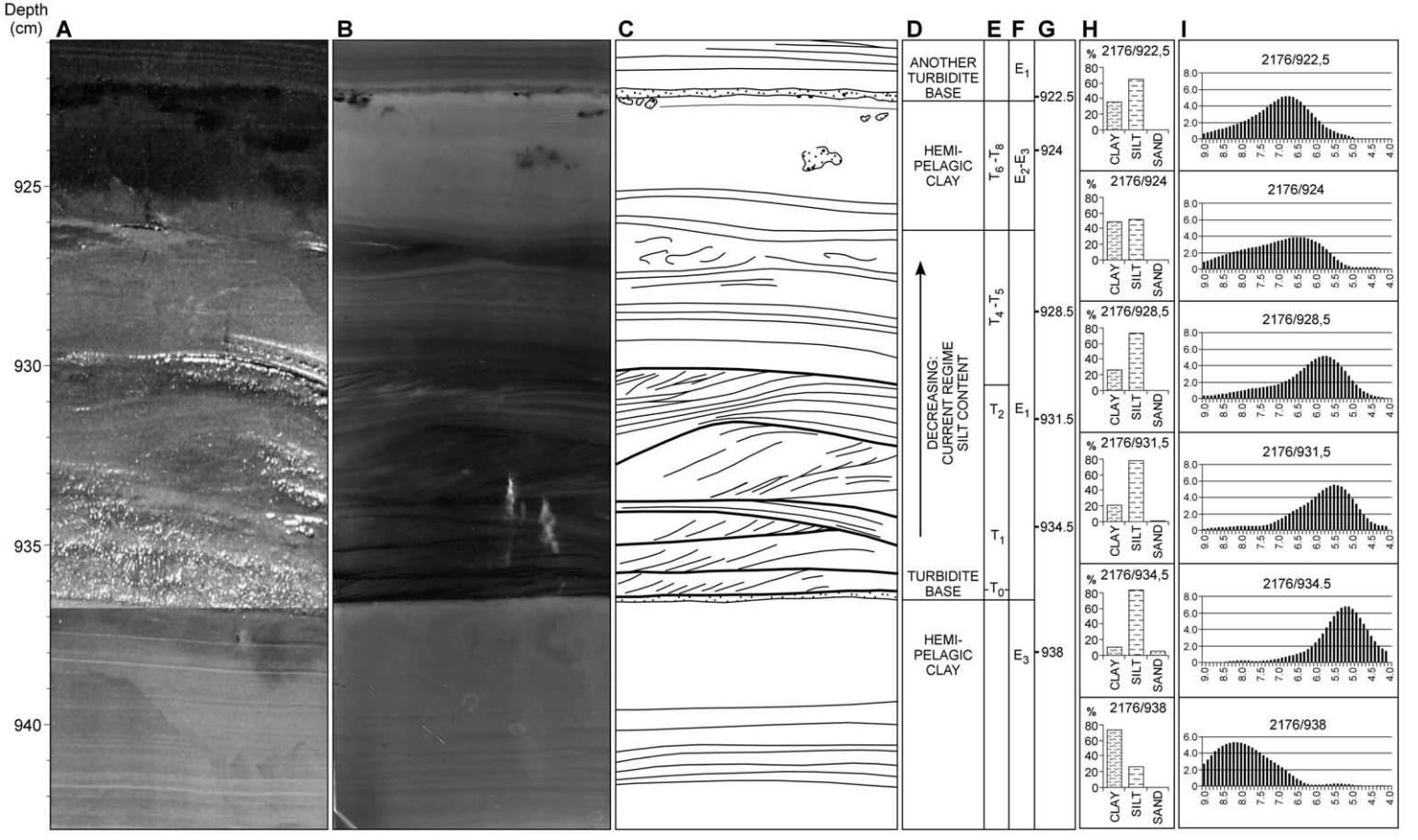

Fig. 3. Selected sample of fining upward cycle facies, core 2176-3, 921–943 cm: (A) photo, (B) X-radiograph, (C) sketch of sedimentary structures, (D) interpretation, (E) classification of turbidite cycle according to Stow and Shanmugam (1980), (F) classification of turbidite cycle according to Piper (1978), (G) sample locations, (H) histograms showing distribution of clay (<2 μm), silt (2–63 μm), and sand (63 μm–2 mm), and (I) histograms showing grain-size distribution (Φ values) of silt.

of sand, but at the base of some cycles, sand values may typically be 5–7%, exceptionally reaching 15–19% in two samples. IRD rarely occur. The sediments show frequent normal grading cycles of approximately 4–20 cm in thickness (Fig. 3). Thin cycles are typically truncated by the next cycle, while the thicker cycles may develop completely into a capping homogenous clay. The thicker cycles typically contain a basal stack of thin (1–2 cm) parallel to sigmoidal cross lamination sets, often eroding and lapping on the set below. This is followed by parallel laminated sets. Then, again slightly cross laminated sets occur, before the lamination changes to planar and fades into homogenous mud. Some wavy laminae may occur among the planar laminae.

The fining upward cycle facies exists more or less across the Amundsen Basin, dominating in the lateral parts of basins, close to the Lomonosov Ridge and Gakkel Ridge (Fig. 2).

3.1.3. Massive diamicton facies

This sedimentary facies is only found in core 2190-1 in three beds in the North Pole core adjacent to Lomonosov Ridge (Fig. 2). The grain sizes range from clay to gravel (Fig. 4). The grain-size distribution typically shows about equal proportions of clay, silt and sand, i.e. between 20 and 40%. The grain-size distribution within the silt shows an even distribution of all silt subfractions (Fig. 4G). IRD is present at all levels, with clasts up to 6 mm diameter. This facies frequently contains characteristic 'lumps' or sediment pellets, similar to those described by Goldschmidt et al. (1992), i.e. aggregates of sediment containing grain sizes from clay to coarse sand or gravel, designated 'sediment pellets'. The diameter of the pellets varies from 4 to 15 mm. Often there is a gradual change in the pellet size, with the larger pellets occurring in the middle part.

3.1.4. Laminated diamicton facies

This facies comprises thin beds and laminae of diamicton interbedded with silt and clay (Fig. 5). The diamicton laminae contain pellets similar to those in the massive diamicton, and may in some cases represent the coarse part in fining upward cycles. The grain-size distributions typically show equal proportions of clay, silt and sand. In the most clayey laminae, the sand percentages are below 10%, with a corresponding increase in clay. IRD grains of sizes up to 1 cm are present throughout the facies. The laminated diamicton facies is abundant on the top of the Lomonosov Ridge, particularly in the upper few metres of the cores 2177-5 and 2185-6 (Fig. 2).

3.2. Core 2190-1 at the North Pole

Core 2190-1 (Figs. 1, 2, and 6) is recovered from the Amundsen Basin at the North Pole. The core is dominated by the fining upward cycle facies, but also includes beds of the homogenous mud and massive diamicton facies. In the fining upward cycle facies, sand typically ranges from 0 to 2%, except for the base of a fining upward cycle at 152 cm, where the sand content reaches 15%. Generally, the combined silt and clay content is close to 100%. The content of silt or clay individually of a sample may be as high as 90% or below 10%, alternating between top ($\approx$90% clay) and bottom ($\approx$90% silt) of the cyclic beds. Single IRD grains are encountered at some levels. Interbedded with the fining upward cycle beds are three massive diamicton beds occurring at 250–307, 390–395 and 410–425 cm, that have between 20 and 40% of any of the grain-size fractions sand, silt and clay, and numerous grains of IRD (Fig. 6). The diamicton beds have sharp lower and upper boundaries (Fig. 4).

The core is grouped into five clay mineral zones (Fig. 6). The upper ca. 100 cm (zone 5) is dominated by illite and has a relatively high percentage of chlorite. Zone 4, 150 cm thick, is smectite-dominated. The difference between zones 5 and 4 does not appear to be correlatable to the different sedimentary facies, as both clay mineral zones are found in fining upward cycle facies. Analyses of separate samples within individual beds in the fining upward cycles did not reveal any systematic differences in the clay mineralogy through the beds/laminae.

Clay mineral zone 3 comprising the massive diamicton facies (250–307 cm) has a remarkably low smectite content and relatively high contents of kaolinite and illite. Zone 2 is quite similar in

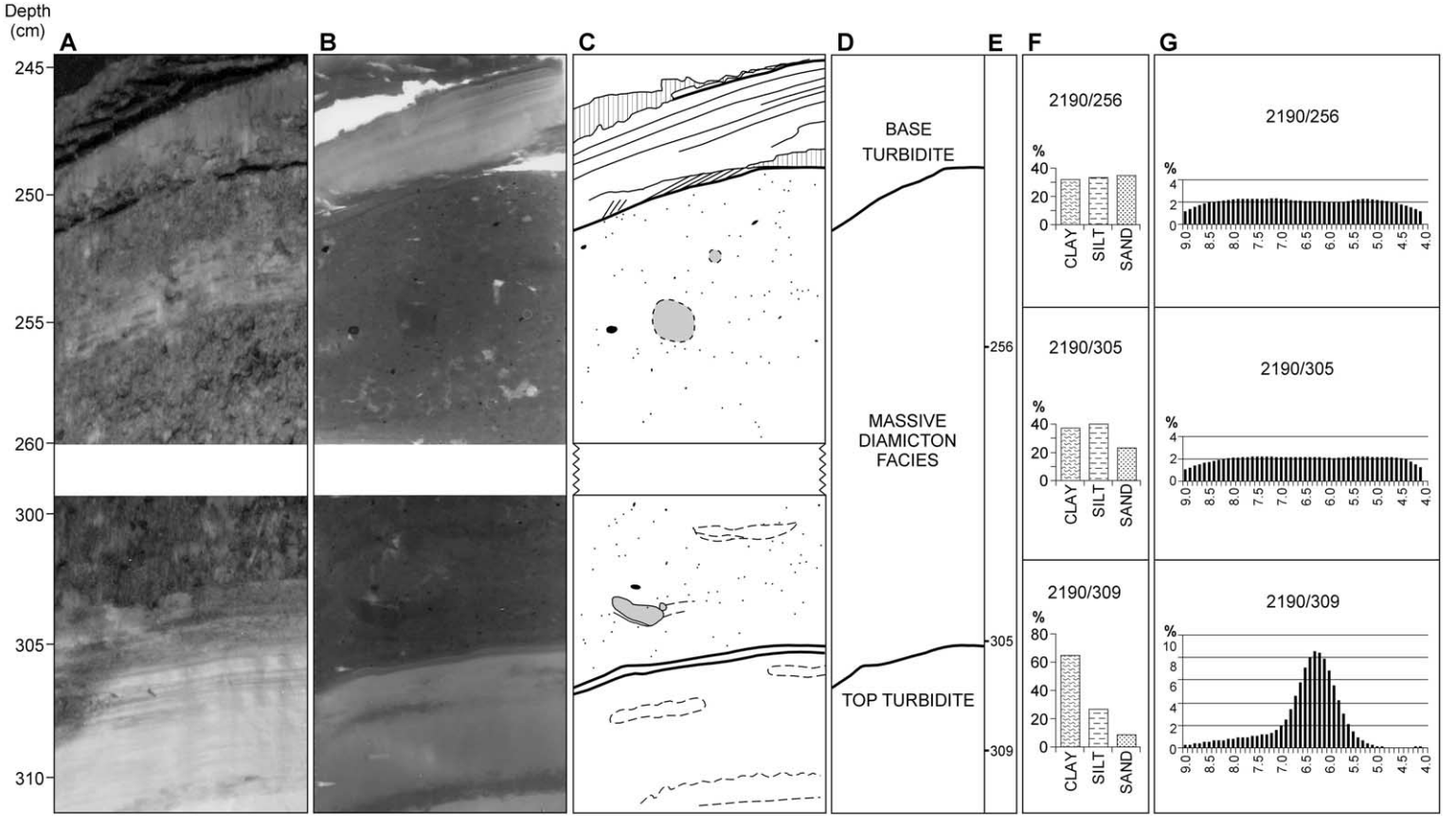

Fig. 4. Selected samples of massive diamicton facies, core 2190-1, 245–260 and 299–312 cm: (A) photo, (B) X-radiograph, (C) sketch of sedimentary structures, (D) interpretation, (E) sample locations, (F) histograms showing distribution of clay (<2 μm), silt (2–63 μm), and sand (63 μm–2 mm), and (G) histograms showing grain-size distribution (Φ values) of silt.

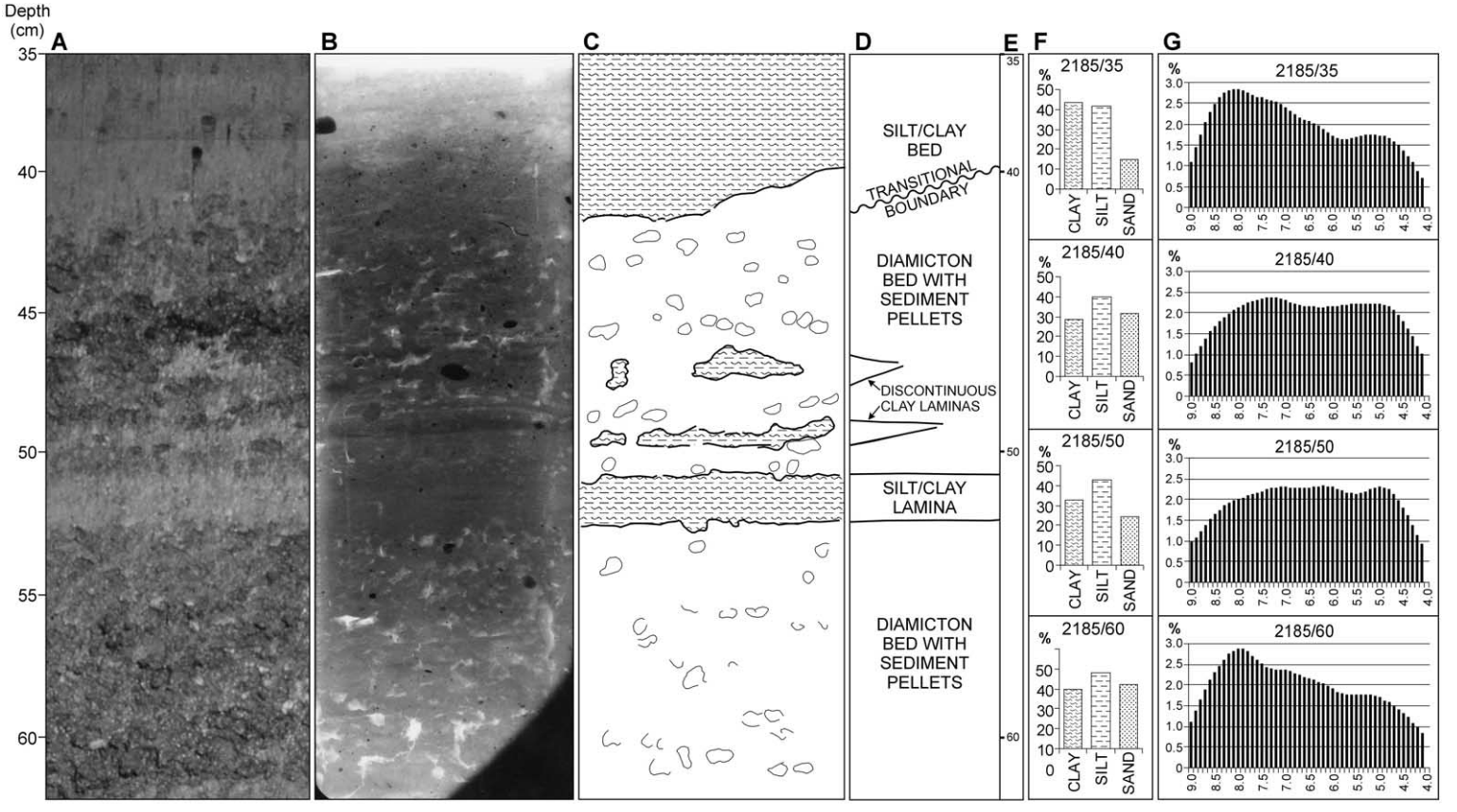

Fig. 5. Selected sample of laminated diamicton facies, core 2185-6, 35–62 cm, from the Lomonosov Ridge: (A) photo, (B) X-radiograph, (C) sketch of sedimentary structures, (D) interpretation, (E) sample locations, (F) histograms showing distribution of clay (<2 μm), silt (2–63 μm), and sand (63 μm–2 mm), and (G) histograms showing grain-size distribution (Φ values) of silt.

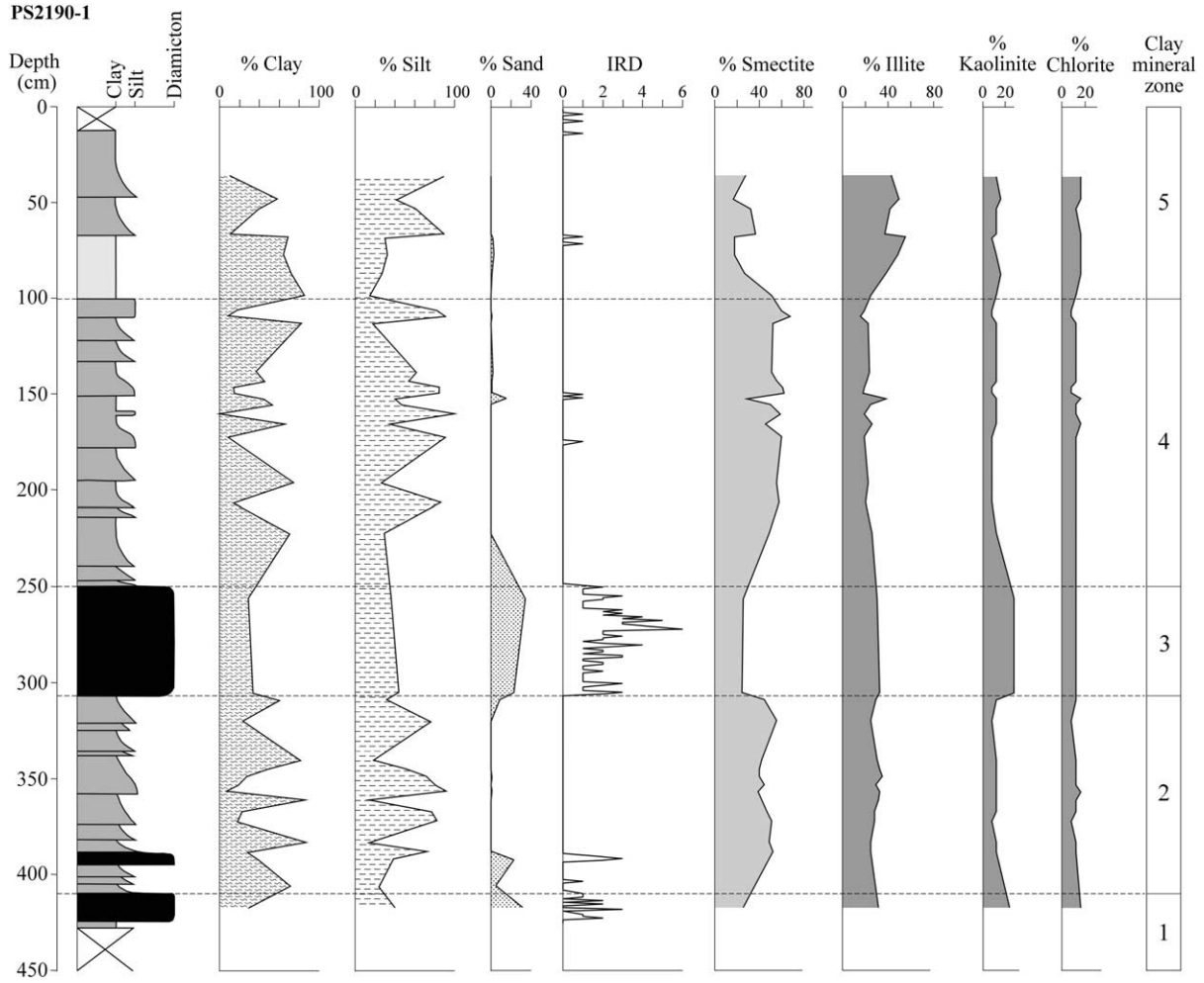

Fig. 6. Lithology, grain-size distribution, IRD frequency (see text on methods), and clay mineralogy of core 2190-1. Shading pattern in the lithostratigraphical column to the left indicate sedimentary facies (see Fig. 2, for legend).

composition to zone 4, and zone 1 bears some resemblance to zone 3.

3.3. Core 2176-3

Core 2176-3, recovered from the central Amundsen Basin, is dominated by fining upward cycle facies (Figs. 2 and 7).

As in core 2190-1, the sand content is low except for one sample (908 cm) containing 19% sand. Elsewhere, the base of the cycles may contain 5–7% sand, but most samples are nearly devoid of sand – even the base of many of the fining upward cycles contain less than 0.1% sand. Clay and silt vary between less than 10% and about 90%, between bottom and top of cycles. The interval between 4.3 and 6.3 m has clay values far above 90%, but the grain-size analyses show fining upward trends in this interval too. This suggests that this interval also could be classified as fining upward cycle facies. However, homogenous mud dominates this interval. Scattered IRD grains are encountered at 303, 409, 416, and 922 cm.

Two clay mineral zones can be distinguished in core 2176-3. The upper 4.2 m shows an illite-dominated illite–chlorite clay mineral association (zone b). Below 4.2 m smectite-dominated clay

mineral association occurs (zone a). Zone b of core 2176-3 resembles zone 5 of core 2190-1, and zone a of 2176-3 resembles zones 4 and 2 of 2190-1, but with reduced smectite values.

3.4. Core 2185-6

Core 2185-6, also described by Spielhagen et al. (1997), is recovered from the crest of the Lomonosov Ridge (Figs. 1, 2, and 8). This core shows a distinct change in sedimentary facies at 3.1 m. Above 3.1 m, the core is dominated by a laminated diamicton facies, comprising beds/laminae of sediment pellets similar to those in the homogenous diamicton facies. These are interbedded with silt/clay laminae. The diamicton beds do some times show gradual transition of the pellets into more muddy sediments, resembling fining upward cycles. Below 3.1 m, the homogenous mud facies dominates. This facies is here sandier and contains more IRD than in the Amundsen Basin.

Below 3.2 m the core has a clay mineral association dominated by illite (Spielhagen et al., 1997). Between 3.2 and ca. 0.5 m, this core is, similar to 2190-1 and 2176-3, rich in smectite. The uppermost ca. 50 cm shows a illite–chlorite clay mineral association similar to the uppermost parts of 2190-1 and 2176-3.

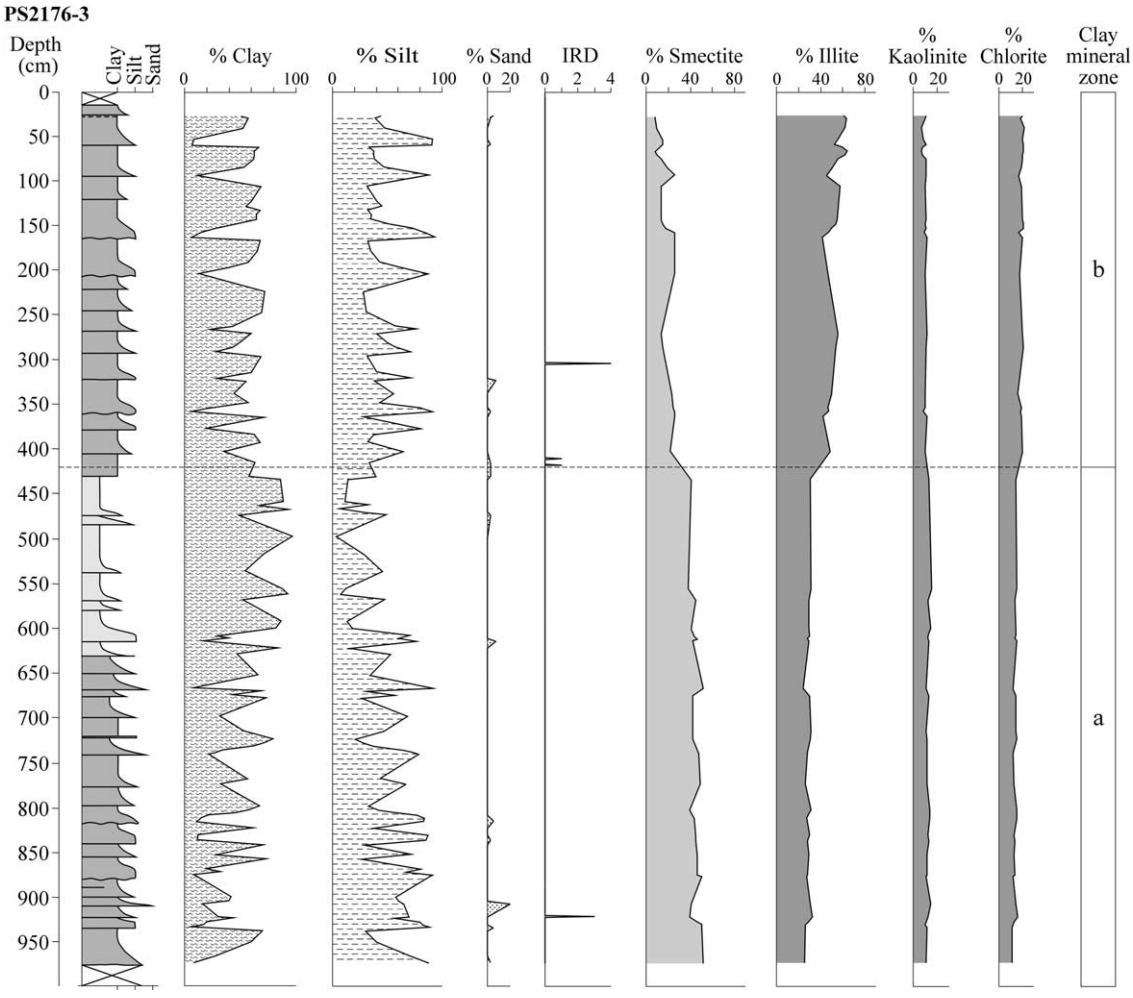

Fig. 7. Lithology, grain-size distribution, IRD frequency (see text on methods), and clay mineralogy of core 2176-3. Shading pattern in the lithostratigraphical column to the left indicates sedimentary facies (see Fig. 2, for legend).

4. Discussion

4.1. Genesis

4.1.1. Homogenous mud facies

The homogenous mud facies depositional environment is interpreted as a hemipelagic clay. It contains no or little IRD within the basin sediments, indicating that deposition from drifting ice is negligible compared to the input from suspended material (hemipelagic settling). Either, practically no ice rafting occurred during the deposition of this sediment facies, or relatively small amounts of IRD may have been deposited and masked by suspension settling or rapid sedimentation. On the Lomonosov Ridge the sandier texture might indicate some winnowing by bottom currents.

4.1.2. Fining upward cycle facies

The fining upward cycle facies consists of beds and lamina of fining upwards medium to fine silt and clay, containing erosional bases. As pointed out by Shanmugam (1997), sediments from different current deposition mechanisms may be difficult to correlate to the exact sedimentary process. The sediment closely resembles the facies T0–T8 (Stow and Shanmugam, 1980) and E1–E3 (Piper, 1978) of fine-grained turbidites (Fig. 3, columns E and F). We therefore infer that this facies represents turbidite deposition. This sediment facies lacks or contains little IRD, indicating that deposition from floating ice is negligible. Probably the IRD input has been masked by rapid turbidite sedimentation.

As mentioned above, clay mineral analyses of individual fining upward cycles did not show any mineralogical variations between the top and bottom of the cycles. Thus, there is no evidence of any difference between clay deposited by turbidity currents, and clay deposited by hemipelagic settling. This indicates that the clay in the turbidites must be of the same origin and composition as any contemporary 'background' sedimentation of hemipelagic clay.

4.1.3. Massive diamicton facies

The massive diamicton facies is only found in core 2190-1, relatively close to the foot of the Lomonosov Ridge (Figs. 2, 4, and 6). Fütterer (1992) does however show similar sediments at the Gakkel Ridge. The sediment occurs in three beds up to 60 cm thick. The texture is similar to the diamicton laminae/beds in the laminated diamicton facies; it contains similar amounts of IRD, and similar sediment pellets. Thus, it is tempting to interpret the massive diamicton facies as a result of more continuous rapid glaciomarine sedimentation events than the laminated diamicton facies (see below), uninterrupted by processes depositing interlaminating mud laminae. However, considering that the rest of core 2190-1 is dominated by turbidite sedimentation, a more likely explanation is that the massive diamicton facies is a result of downslope transport of the laminated diamicton facies from the adjacent Lomonosov Ridge as submarine debris flows. The sediment pellets have been preserved, while the sediments of the muddy laminae have been separated into suspension, or have been mixed into the homogenous massive diamicton. Jakobsson (1999) describes, based on seismic records, erosion of about 50 m of the sediment stratigraphy on the Lomonosov Ridge. The crest of the Lomonosov Ridge is interpreted to be covered by glacial flutes derived from a grounded glacier during Saalian or older ice ages (Polyak et al., 2001). The present slope of the Lomonosov Ridge facing the Amundsen Basin is marked by several gullies (Polyak et al., 2001, Fig. 4). These gullies testify to gravity flows released from the top of the Lomonosov Ridge. Probably the massive diamictons are derived from such gravity flows.

4.1.4. Laminated diamicton facies

The laminated diamicton facies, found in cores 2177-5 and 2185-6 on the crest of the Lomonosov Ridge, shows laminae of sandy mud interlaminated with laminae of diamicton containing sediment pellets and clasts. Similar sediment pellets were described by Goldschmidt et al. (1992) who concluded that the pellets were generated as cryoconites in sea-ice or icebergs. This, together with the presence of IRD in all samples, indicates that deposition from sea-ice or icebergs was an important sedimentary process. The laminated structure

of the sediment may be due to winnowing by bottom currents.

4.2. Chronology and sedimentation rates

We infer that the shift in clay mineral content from smectite-dominated to illite–chlorite, i.e. zone 5/4 at 100 cm in core 2190-1 and zone a/b at 420 cm in core 2176-3, is synchronous. A similar distinct shift in clay mineralogy is found at approximately 50 cm in core 2185-6 (Fig. 8; Spielhagen et al., 1997). When studying the beryllium curve, correlated to marine oxygen isotope stages in fig. 2 of Spielhagen et al. (1997), the age of this shift seems to occur during their inferred isotope stage 4, i.e. approximately 80 ka BP. Jakobsson et al. (2000) suggest a different age model in a correlatable nearby core. They indicate an age of about 150 ka BP for a stratigraphic horizon dated to 700 ka BP by Spielhagen et al. (1997). Assuming the same relative sedimentation rates for the two age models, this gives an age of 17 ka BP for the mentioned clay mineral boundary. Recently, Spielhagen (autoref: EUG-meeting 2001) revised his age model, and supported the model of Jakobsson et al. (2000).

Using the Jakobsson et al. (2000) age model, the sedimentation rates for the intervals represent-

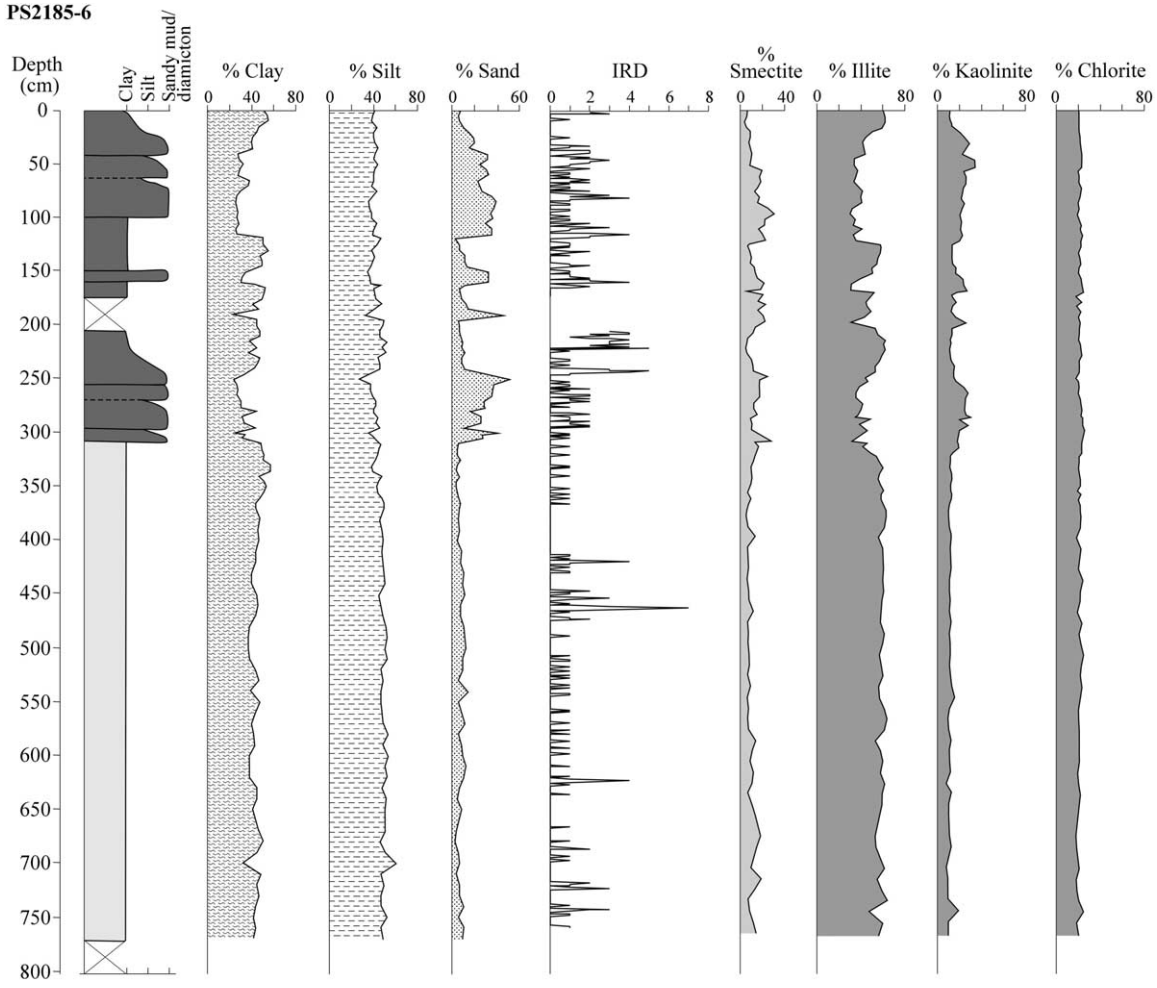

Fig. 8. Lithology, grain-size distribution, IRD frequency (see text on methods), and clay mineralogy of core 2185-6. Shading pattern in the lithostratigraphical column to the left indicates sedimentary facies (see Fig. 2, for legend).

ing the last 17 000 yr will be: 29 mm/ka (core 2185-6), 59 mm/ka (core 2190-1), and 247 mm/ka (core 2176-3).

Previously estimated sedimentation rates for the Arctic Ocean in the Amerasian Basin in pelagic and IRD-controlled sedimentary environments (Clark et al., 1980; Herman and Hopkins, 1980; Darby et al., 1989; Grantz et al., 1996; Darby et al., 1997) are 1–5 mm/ka. The high sedimentation rates on top of the Lomonosov Ridge, 29 mm/ka, found by us are comparable to the Amerasian sedimentation rates by Sejrup et al. (1984).

The two cores from the Amundsen Basin (2190-1 and 2176-3) have quite higher sedimentation rates than the ridge core, as can be expected in a turbidite prone environment. High sedimentation rates in turbidite sediments are also found by Grantz et al. (1996) on the Canada Abyssal Plain of the Amerasian basin. The differences between 2190-1 (59 mm/ka) and 2176-3 (247 mm/ka) may be due to the better exposed location of core 2176-3 than 2190-1. The latter is located in a slightly sheltered embayment at the foot of the Lomonosov Ridge (Fig. 1).

4.3. Provenance

The following discussion of provenance is based on modern clay mineral distribution in surface samples of the Eurasian Arctic Ocean and continental margin as described by Wahsner et al. (1999).

The clay mineralogy does not seem to vary between the homogenous mud facies and the fining upward cycle facies. This indicates that sediments deposited by different processes originate from the same source area.

The uppermost part of each core, where clay mineralogy data are available, shows an illite–chlorite association. This clay mineral association has several possible source areas. The Barents Sea continental shelf including Svalbard is one possible source area. Another possibility is Greenland (Wahsner et al., 1999).

Since these parts of the cores are considered to be deposited during the Weichselian–Holocene, (see above) the Barents shelf is a possible provenance area. The Barents Sea continental shelf was glaciated by a grounded ice sheet at least twice during the actual period (Mangerud et al., 1998; Landvik et al., 1998). During those glaciations sediments from the shelf must have been transported by icebergs and glacial meltwater to the Arctic Ocean Basin margins and Lomonosov Ridge, and later redeposited by turbidity currents.

Based on the observation of the sea floor morphology, the Greenland continental margin also stands out as another important source area. Svendsen (1997) observed channels on the deep-sea floor of the Amundsen Basin. The geometry of the channels and their levels have the shape one would expect for channels serving as pathways for turbidite currents flowing east from the Greenland continental margin towards the North Pole, influenced by Coriolis force. This may indicate that during the deposition of the fining upward cycle facies in the uppermost parts of the cores, the bottom current sediment transport was dominated by turbidite currents from northern Greenland.

The smectite-dominated portions of the cores (zones 2 and 4 in core 2190-1 and zone a in core 2176) indicate the eastern Laptev Sea and/or Kara Sea as the most likely sediment source. Wahsner et al. (1999) and Schoster et al. (2000) have shown that those two shelf areas are characterised by increased content of smectite derived from the hinterland. The Laptev Sea is a very obvious source for sediments to the Amundsen Basin. Sea-ice formed in that area would drift straight into the Transpolar Drift and across the study area. Rivers crossing the shelf would feed the continental slope and thereafter gravity flows could take the sediments into the Amundsen Basin.

The massive diamicton facies exhibits quite different kaolinite rich clay mineralogy (zones 3 and 1 in core 2190), suggesting that this sediment facies may have a different provenance. Kaolinite is common on many of the shelves surrounding the Arctic Ocean, so the exact provenance is not revealed by this observation alone. As mentioned above, this facies does most likely represent sediments derived by gravity flows from the Lomonosov Ridge.

The shift between clay mineralogy zones a and

b in core 2176-3, and respectively 2+4 and 5 in 2190-1, may indicate a change in spatial and temporal gravity flow regime and or ocean bottom currents during the Late Weichselian (about 17 ka BP according to the Jakobsson et al. (2000) age model). The change might relate to the deglaciation history and the related sea level history of the continental shelves surrounding the Arctic Ocean. However, a better understanding will be achieved when a fixed chronology is established.

5. Conclusions

1: Four main sedimentary facies have been identified in the Amundsen Basin and Lomosov Ridge: (1) homogenous mud facies, (2) fining upward cycle facies, (3) massive diamicton facies, and (4) laminated diamicton facies. Deposition by turbidite currents is the quantitative most important process in the Amundsen Basin, followed by hemipelagic settling. Ice rafting is negligible.

2: Using age models of Jakobsson et al. (2000) we find that sedimentation rates during the last clay mineral zone (17 ka BP) in the turbidite-dominated Amundsen Basin are up to almost 10 times higher than the sedimentation rate encountered on the Lomonosov Ridge and in pelagic and IRD-controlled sedimentary environments of the Amerasian Basin. Being a turbidite-dominated environment this may be expected, and these sedimentation rates are still far below the sedimentation rates of turbidite sediments described by Grantz et al. (1996) on the Canada Abyssal Plain of the Amerasian basin.

3: Three different clay mineralogy associations are found: (1) illite–chlorite association, (2) smectite association, and (3) kaolinite–illite association. The latter is related to the massive diamicton facies, while the two first are related to fining upward cycle facies and homogenous clay facies.

4: The illite–chlorite association is probably derived from the Barents Sea and Greenland margin; the smectite association from the Kara and Laptev Sea and the kaolinite association from the Lomonosov Ridge.

5: The change in clay mineralogy between different clay mineral zones indicates a spatial and temporal change in the gravity flow activity and bottom current regime. This is probably related to the glaciation and sea-level history of the continental shelves surrounding the Arctic Ocean.

Acknowledgements

We thank the chief scientist Prof. D.K. Fütterer, captain E.-P. Greve, and crew of RV *Polarstern* for their support during cruise Arctic '91. Thanks to scientific and technical personnel at Department of Geology, University of Tromsø, and Alfred Wegener Institut, Bremerhaven, for discussions, cooperation and assistance with laboratory analyses. AWI is also thanked for making material and data available. Financial support was contributed by The Norwegian Research Council. We are grateful to Jan P. Holm, University of Tromsø, who made most of the illustrations.

References

Aagaard, K., Carmack, E., 1994. The Arctic Ocean and climate: A perspective. In: Johannessen, J., Muench, R.D., Overland, J.E. (Eds.), The Polar Oceans and Their Role in Shaping the Global Environment. Geophysical Monograph 85, American Geophysical Union, pp. 4–20.

Clark, D.L., 1990. Arctic Ocean ice cover; Geologic history and climatic significance. In: Grantz, A., Johnson, L., Sweeney, J.F. (Eds.), The Geology of North America, Vol. L, The Arctic Ocean Region. Geological Society of America, Ch. 4, pp. 53–62.

Clark, D.L., Whitman, R.R., Morgan, K.A., Mackey, S.D., 1980. Stratigraphy and glacial-marine sediments of the Amerasian Basin, central Arctic Ocean. Geological Society of America Special Paper 181, 57 pp.

Darby, D.A., Naidu, A.S., Mowatt, T.C., Jones, G., 1989. Sediment composition and sedimentary processes in the Arctic Ocean. In: Herman, Y. (Ed.), The Arctic Seas, Ch. 24. Van Nostrand Reinhold, New York, pp. 657–712.

Darby, D.A., Bischof, J.F., Jones, G.A., 1997. Radiocarbon chronology of depositional regimes in the western Arctic Ocean. Deep-Sea Res. II 44, 1745–1757.

Eidnes, S.E., 1993. Geostandard. En geologisk standard til bruk i petroleumsvirksomheten (A geological standard for use within the petroleum industry). Norwegian Petroleum Directorate Bull. 7, 160 pp.

Fütterer, D.K., 1992. ARCTIC '91: The expedition ARK-VIII/3 of RV *Polarstern* in 1991. Berichte zur Polarforschung 107, 267 pp.

Goldschmidt, P.M., Pfirman, S.L., Wollenburg, I., Henrich, R., 1992. Origin of sediment pellets from the Arctic seafloor: sea ice or icebergs? Deep-Sea Res. 39 (Suppl. 2), S539–S565.

Gordienko, P.A., Laktionov, A.F., 1969. Circulation and physics of the Arctic Basin waters. Annuals of the International Geophysical Year. Oceanography 46, 94–112.

Grantz, A., Phillips, R.L., Mullen, M.W., Starratt, S.W., Jones, G.A., Naidu, A.S., Finney, B.P., 1996. Character, paleoenvironment, rate of accumulation, and evidence for seismic triggering of Holocene turbidites, Canada Abyssal Plain, Arctic Ocean. Mar. Geol. 133, 51–73.

Grobe, H., 1987. A simple method for the determination of ice-rafted debris in sediment cores. Polarforschung 57, 123–126.

Herman, Y., Hopkins, D.M., 1980. Arctic oceanic climate in late Cenozoic time. Science 209, 557–569.

Jakobsson, M., 1999. First high-resolution chirp sonar profiles from the central Arctic Ocean reveal erosion of Lomonosov Ridge sediments. Mar. Geol. 158, 111–123.

Jakobsson, M., 2000. Mapping the Arctic Ocean: Bathymetry and Pleistocene Paleoceanography. Medd. Stockholms Universitets Institution för Geologi og Geokemi, No. 306.

Jakobsson, M., Løvlie, R., Al-Hanbali, H., Arnold, E., Backman, J., Mörth, M., 2000. Manganese and color cycles in Arctic Ocean sediments constrain Pleistocene chronology. Geology 28, 23–63.

Johnson, L., Grantz, A., Weber, J.R., 1990. Bathymetry and physiography. In: Grantz, A., Johnson, L., Sweeney, J.F. (Eds.), The Geology of North America, Vol. L, The Arctic Ocean Region. Geological Society of America, Ch. 5, pp. 63–75.

Jones, E.P., Rudels, B., Anderson, L.G., 1995. Deep waters of the Arctic Ocean: Origin and circulation. Deep-Sea Res. I 45, 737–760.

Landvik, J.Y., Bondevik, S., Elverhøi, A., Fjeldskaar, W., Mangerud, J., Salvigsen, O., Siegert, M.J., Svendsen, J.I., Vorren, T.O., 1998. The last glacial maximum of Svalbard and the Barents Sea area: Ice sheet extent and configuration. In: Elverhøi, A., Dowdeswell, J., Funder, S., Mangerud, J., Stein, R. (Eds.), Glacial and Oceanic History of the Polar North Atlantic Margins. Quat. Sci. Rev. 17, 43–75.

Mangerud, J., Dokken, T., Hebbeln, D., Heggen, B., Ingolfsson, O., Landvik, J.Y., Mejdahl, V., Svendsen, J.I., Vorren, T.O., 1998. Fluctuations of the Svalbard-Barents Sea ice sheet during the last 150,000 years. In: Elverhøi, A., Dowdeswell, J., Funder, S., Mangerud, J., Stein, R. (Eds.), Glacial and Oceanic History of the Polar North Atlantic Margins. Quat. Sci. Rev. 17, 11–42.

Nürnberg, D., Wollenburg, I., Dethleff, D., Eicken, H., Kassens, H., Letzig, T., Reimnitz, E., Thiede, J., 1994. Sediments in Arctic sea ice: Implications for entrainment, transport and release. In: Thiede, J., Vorren, T., Spielhagen, R.F. (Eds.), Arctic Ocean Marine Geology. Mar. Geol. 119, 185–214.

Pfirman, S.L., Kögeler, J., Anselme, B., 1995. Coastal environments of the western Kara and Barents seas. Deep-Sea Res. II 42, 1391–1412.

Pfirman, S.L., Colony, R., Nürnberg, D., Eicken, H., Rigor, I., 1997. Reconstructing the origin and trajectory of drifting Arctic sea ice. J. Geophys. Res. 102, 12575–12586.

Phillips, R.L., Grantz, A., 2001. Regional variations in provenance and abundance of ice-rafted clasts in Arctic Ocean sediments: implications for the configuration of late quaternary oceanic and atmospheric circulation in the Arctic. Mar. Geol. 172, 91–115.

Piper, D.J.W., 1978. Turbidites, muds and silts on deep-sea fans and abyssal plains. In: Stanley, D.J., Kelling, G. (Eds.), Sedimentation in Submarine Canyons, Fans and Trenches. Dowden, Hutchinson and Ross, Stroudsburg, PA, pp. 163–175.

Polyak, L., Edwards, M.H., Coakley, B.J., Jakobsson, M., 2001. Ice shelves in the Pleistocene Arctic Ocean inferred from glaciogenic deep-sea bedforms. Nature 410, 453–457.

Schoster, F., Behrends, M., Müller, C., Stein, R., Wahsner, M., 2000. Modern river discharge and pathways of supplied material in the Eurasian Arctic Ocean: evidence from mineral assemblages and major and minor element distribution. Int. J. Earth Sci. 89, 486–495.

Sejrup, H.P., Miller, G.H., Brigham-Grette, J., Løvlie, R., Hopkins, D., 1984. Amino acid epimerization implies rapid sedimentation rates in Arctic Ocean cores. Nature 310, 772–775.

Shanmugam, G., 1997. The Bouma sequence and the turbidite mind set. Earth Sci. Rev. 42, 201–229.

Spielhagen, R.F., Bonani, G., Eisenhauer, A., Frank, M., Friedrichs, T., Kassens, H., Kubik, P.W., Mangini, A., Nørgaard-Pedersen, N., Nowaczyk, N.R., Schäper, S., Stein, R., Thiede, J., Tiedemann, R., Wahsner, M., 1997. Arctic Ocean evidence for late Quaternary initiation of northern Eurasian ice sheets. Geology 25, 783–786.

Stein, R., 1985. Rapid grain-size analyses of clay and silt fraction by Sedigraph 5000D: Comparison with Coulter counter and Atterberg methods. J. Sediment. Petrol. 55, 590–593.

Stein, R., Grobe, H., Wahsner, M., 1994. Organic carbon, carbonate and clay mineral distribution in eastern central Arctic Ocean sediments. In: Thiede, J., Vorren, T., Spielhagen, R.F. (Eds.), Arctic Ocean Marine Geology. Mar. Geol. 119, 269–285.

Stow, D.A.V., Shanmugam, G., 1980. Sequence of structures in fine-grained turbidites: comparison of recent deep-sea and ancient flysch sediments. Sediment. Geol. 25, 23–42.

Svendsen, O., 1997. En geofysisk tolkning av sedimentasjonshistorien i Amundsenbassenget. Unpubl. Cand. Scient. Thesis, University of Tromsø.

Wahsner, M., Müller, C., Stein, R., Ivanov, G., Levitan, M., Shelekhova, E., Tarasov, G., 1999. Clay-mineral distribution in surface sediments of the Eurasian Arctic Ocean and continental margin as indicator for source areas and transport pathways – a synthesis. Boreas 28, 215–233.

Wolf-Welling, T.C.W., Cremer, M., O'Connel, S., Winkler, A., Thiede, J., 1996. Cenozoic Arctic gateway paleoclimate variability: Indications from changes in coarse-fraction composition (ODP Leg 151). In: Thiede, J., Myhre, A.M., Firth, J. et al. (Eds.), Proc. ODP, Sci. Results, 151. ODP, College Station, TX.